IJARST

International Journal of Advanced Research in Science and Technology

https://doi.org/10.62226/ijarst20262646

ISSN 2319 – 1783 (Print)

ISSN 2320 – 1126 (Online)

Design and Analysis of Modified Bridgeless AC to DC Interleaved ZETA Converter for Electric Vehicle Charging Application

Thangasankaran R[1], Dr S Parthasarathy[2], Rageshwaran J K[3], Bharath Kumar P G[3], Janagivarman B[3], Murugan I[3]

[1]Asst. Professor, Dept of EEE, K.L.N. College of Engineering, Sivagangai, Tamil Nadu, India

[2]Professor, Dept of EEE, K.L.N. College of Engineering, Sivagangai, Tamil Nadu, India

[3]UG Scholars, Dept of EEE, K.L.N. College of Engineering, Sivagangai, Tamil Nadu, India

rageshwaran2005@gmail.com, thangasankaranr@gmail.com

ARTICLEINFO

Article history:

Received 23 Apr 2026
Accepted 29 Apr 2026
Available online 06 May 2026

Keywords:

Bridgeless converter; Electric Vehicle (EV) charger; Interleaved ZETA converter; Power Factor Correction (PFC); PI controller; MATLAB/Simulink; Continuous Conduction Mode (CCM); Total Harmonic Distortion (THD); PWM control

Indexed in:

and in major libraries

ABSTRACT

Effective AC-DC power conversion with low losses and enhanced power quality is a fundamental requirement for electric vehicle (EV) charging systems. Conventional EV chargers that employ diode bridge rectifiers suffer from significant conduction losses due to two simultaneous diode voltage drops (~1.4 V per cycle), increased input current ripple, elevated total harmonic distortion (THD), and degraded overall efficiency — all of which become increasingly severe at higher power levels. This paper presents the design and analysis of a Modified Bridgeless AC-DC Interleaved ZETA Converter for EV off-board charging applications. The proposed topology eliminates the conventional diode bridge by allowing the AC input to be processed directly through controlled MOSFET switches, thereby removing conduction losses and the dead-band distortion near zero crossings. Two ZETA converter stages operate in parallel with 180° phase-shifted PWM signals, distributing current stress uniformly and reducing the effective ripple frequency to 40 kHz — twice the switching frequency. The converter is rated at 300 W with a 60 V DC regulated output from a 230 V AC (RMS), 50 Hz grid supply at a switching frequency of 20 kHz. A PI controller provides precise voltage regulation. Performance is validated using MATLAB/Simulink 2024a under open-loop and closed-loop control, along with static (supply voltage variation) and dynamic (load variation) analyses. Results confirm near-unity power factor, THD compliant with IEC 61000-3-2, fast transient recovery, and stable DC output — demonstrating the proposed converter as a reliable solution for modern EV charging infrastructure.

1. Introduction:

The rapid global adoption of electric vehicles (EVs) has created an urgent need for efficient, reliable, and power-quality-compliant AC-DC conversion systems. EV chargers must convert grid-supplied alternating current (AC) into regulated direct current (DC) for battery management systems while meeting international standards on power factor, harmonic distortion, and electromagnetic interference. Conventional EV charging systems rely on a full-wave diode bridge rectifier followed by a single DC-DC conversion stage — an architecture that, while functionally adequate, introduces several performance penalties that become increasingly problematic at higher power levels. [29,30]

The central limitation of diode bridge rectifiers is conduction loss. Two diodes conduct simultaneously in each half-cycle, each introducing a forward voltage drop of approximately 0.7 V — a combined 1.4 V drop per cycle. At the rated output current of 5 A, this alone accounts for 7 W of wasted power in the rectification stage. Furthermore, the bulk capacitor placed directly after the bridge rectifier charges only during the voltage peaks, drawing current from the supply in narrow, high-amplitude pulses rather than as a continuous sinusoidal waveform. This results in a poor input power factor (typically 0.5–0.65) and elevated THD in the input current — in violation of IEC 61000-3-2 harmonic current emission limits. [28] Single-stage DC-DC converters further exacerbate the problem by generating higher ripple current, increasing stress on switching devices and degrading battery longevity. [31]

This paper presents the design and analysis of a Modified Bridgeless AC-DC Interleaved ZETA Converter that addresses all these limitations

simultaneously. The bridgeless configuration eliminates the diode bridge, allowing the AC input to be processed directly by controlled MOSFET switches — one pair per AC half-cycle. [14] This removes the two-diode conduction loss and eliminates the zero-crossing dead-band distortion inherent to bridge rectifiers. The interleaved topology deploys two ZETA converter stages in parallel with 180° phase-shifted PWM switching, causing ripple currents to partially cancel at both input and output, halving ripple amplitude and doubling the effective ripple frequency to 40 kHz. The converter is rated at 300 W, delivering 60 V DC from a 230 V AC (RMS) supply at 20 kHz switching frequency. A PI controller enforces precise closed-loop voltage regulation. [16,24]

The remainder of this paper is structured as follows: Section II reviews relevant prior literature; Section III surveys existing EV charger converter topologies; Section IV describes the proposed converter — block diagram, circuit operation, and modes; Section V presents design equations and component calculations; Section VI analyses MATLAB/Simulink simulation results; and Section VII concludes the paper.

2. Related Work:

A growing body of research has progressively developed converter topologies for power quality improvement and EV charging applications. The following review traces the key contributions that directly motivate the proposed system.

B. N. Singh and B. Singh [1] presented a conventional ZETA converter for power quality improvement operating in Discontinuous Conduction Mode (DCM). Both step-up and step-down conversion were demonstrated with positive output polarity. The DCM operation naturally improves input power factor and reduces THD, establishing the ZETA converter as a viable PFC topology and providing the foundational reference for this work.

Jothimani, Gnanavadivel, Palanichamy, Natarajan, and Thangasankaran [23] proposed a single-phase front-end modified interleaved Luo power factor correction converter for on-board EV charger applications. The interleaved Luo topology demonstrated inherent PFC capability with reduced input current ripple and improved power quality, providing important insights into interleaved PFC converter design for EV charging that directly inform the proposed interleaved ZETA approach.

J. S. Alagesan et al. [5] demonstrated an interleaved ZETA converter for photovoltaic applications using two parallel stages with phase-shifted switching signals. The interleaving technique reduced output current ripple, improved voltage regulation, and distributed thermal stress more uniformly across switching devices compared to a single-stage ZETA.

M. H. Ayalani and S. N. Pandya [7] evaluated an interleaved ZETA converter specifically in EV charging applications. Their results confirmed enhanced power conversion efficiency, reduced ripple current, and stable output voltage — verifying the suitability of the interleaved architecture for demanding EV charger requirements.

Thangasankaran and Parthasarathy [30] performed a Proteus/Simulink analysis of a rectifier-based electric vehicle charger circuit, demonstrating simulation-based validation methodology for EV charger topologies. In a related study, **Thangasankaran, Parthasarathy et al.** [31] presented a MATLAB/Simulink analysis of a ripple-free high-efficiency buck-boost type converter for EV charging and controlling applications, highlighting the superiority of advanced converter topologies over simple rectifier-based approaches for EV charging.

Gnanavadivel, Thangasankaran et al. [24] conducted a performance analysis of PI controller and PR controller based three-phase AC-DC boost converter with space vector PWM. The study established the superiority of PI control for steady-state voltage regulation, and the inferiority of derivative action in switching converter environments — findings that directly justify the PI controller selection in the proposed system.

Lakshmi, Thangasankaran, and Gnanavadivel [25] evaluated the performance of a fuzzy-controlled single-phase PWM rectifier, demonstrating intelligent controller approaches for improving power factor and reducing harmonics in single-phase AC-DC conversion. **Alagesan, Thangasankaran, and Karthikeyan** [28] studied harmonic content elimination using three-phase PWM rectifiers and phase-controlled rectifiers, quantifying the THD reduction achievable through PWM-based rectification compared to conventional phase-controlled approaches.

Thangasankaran, Jaya Christa, Gnanavadivel, and Senthil Kumar [27] presented the design and analysis of a negative output Luo converter for power quality enhancement.

Thangasankaran, Shanthini, and Parthasarathy [33] designed an AC-DC interleaved negative output Ćuk converter for power quality enhancement, and **Siddharthan, Thangasankaran, Gnanavadivel, and Jaya Christa** [34] analysed a DC-DC Ćuk converter with interleaved topology. These works collectively demonstrate that interleaved converter architectures — applied across ZETA, Luo, and Ćuk topologies — consistently deliver superior power quality, reduced ripple, and improved thermal distribution compared to single-stage designs.

Shanthi, Kalyani, and Thangasankaran [26] analysed performance of speed control with sinusoidal PWM and space vector PWM-fed voltage source inverters, providing comparative insights into PWM modulation strategies that underpin the switching control in the proposed converter.

Thangasankaran [32] presented the design and analysis of an AC to DC SEPIC converter for low power applications, providing a comparative baseline for understanding SEPIC behaviour relative to the ZETA topology adopted in this work.

B. Singh and U. Sharma [14] introduced a bridgeless ZETA converter for power factor correction that

eliminates the diode bridge entirely. Experimental results demonstrated reduced conduction losses, improved power factor, decreased THD, and superior thermal performance relative to conventional bridge-based converters — directly motivating the bridgeless topology in this work.

R. Thangasankaran et al. [16] presented a high-efficiency AC-DC converter using an interleaved ZETA topology for EV off-board charging. The converter achieves inherent PFC in DCM with input THD below 2%, compliant with IEC 61000-3-2 standards. Simulation results show 1% voltage ripple and 2% current ripple at 60 V DC. This work is the closest direct precedent to the proposed system.

Thangasankaran, Patnaik, Bhuvanesh et al. [29] investigated the application of novel converters for hybrid renewable energy systems, highlighting the growing relevance of advanced power electronic converter topologies in sustainable energy applications — an application space to which the proposed EV charger directly contributes.

3. Existing Converter Topologies for EV Charging:

A. AC-DC Converter Topologies

Active Front End (AFE) converters use IGBTs or MOSFETs to achieve high efficiency, bidirectional power flow, and power factor correction. They are deployed in high-power off-board charging stations (22 kW+) where low harmonics and near-unity power factor are mandatory, and where V2G (Vehicle-to-Grid) capability is required. [29] Isolated AC-DC converters use high-frequency transformers to provide galvanic isolation between the grid and the EV battery, enhancing safety in both on-board and off-board chargers for high-power fast-charging scenarios. Single-phase PWM rectifiers represent a step forward from diode-bridge approaches by enabling controllable power factor and reduced harmonic content. [25] However, both AFE and isolated topologies add significant complexity and cost. For the 300 W application targeted in this work, a non-isolated bridgeless topology is sufficient and more efficient.

B. DC-DC Converter Topologies

Buck converters step down DC voltage and are used in Level 1/2 charging but cannot step up. Boost converters step up but cannot step down. Bidirectional buck-boost converters support both V2G and charging but require a full bridge driver. Ripple-free buck-boost type converters have been specifically developed for EV charging to achieve both step-up and step-down with minimised input current ripple. [31] Among non-isolated topologies, the ZETA converter is distinguished by its ability to both step up and step down, maintain a non-inverting output polarity (unlike the Ćuk converter), exhibit continuous input current (unlike SEPIC), and achieve high PFC capability.[1,14]

C. Comparative Analysis: SEPIC, ZETA, and Luo Converters

Table 1 presents a comparative analysis of the three principal non-isolated, non-inverting converter topologies most relevant to EV charger applications. Prior work on the SEPIC topology for AC-DC conversion [32] has established its limitations in THD and efficiency relative to ZETA. The interleaved Luo converter, while offering high PFC capability, exhibits output polarity flexibility at the cost of higher design complexity. [23,27] The ZETA converter demonstrates the most favourable combination of low THD (<2%), high efficiency (90–94%), low current and voltage ripple, and low component stress — confirming the design selection.

Table 1. Comparative Analysis of SEPIC, ZETA, and Luo Converters

Parameter	SEPIC	ZETA	Luo
Voltage Gain (Vout/Vin)	D/(1-D)	D/(1-D)	D/(1-D)
Output Polarity	Positive	Positive	Positive or Negative
PFC Capability	Moderate	High	High
THD	3–6%	<2%	<3%
Efficiency	85–90%	90–94%	88–92%
Input Current Ripple	High	Low	Medium
Voltage Ripple	Medium	Low	Low
Component Stress	Moderate	Low	Low
Typical Application	LED drivers, power supplies	EV chargers, PFC	DC microgrids, industrial drives

4. Proposed Methodology:

A. Block Diagram

The proposed system processes 230 V AC (RMS) through four functional stages. The bridgeless rectifier directly converts AC to pulsating DC using controlled MOSFETs — one set per half-cycle — without a diode bridge. [14,30] The rectified pulsating DC feeds the two-stage interleaved ZETA converter, which provides regulated DC-DC conversion at 180° phase offset. An

output LC filter smooths the output. A closed-loop PI controller senses the 60 V output, computes the error relative to the reference, and dynamically adjusts the PWM duty cycle to maintain regulation under varying load and supply conditions. [24]

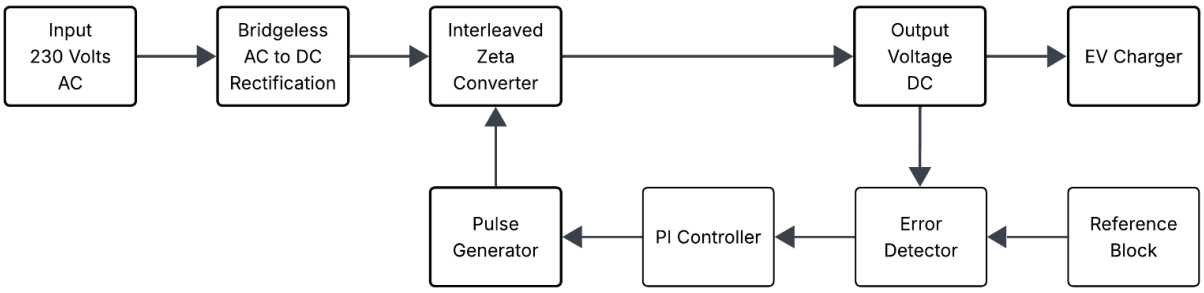

[Fig. 1 — Block Diagram of the Proposed Converter]

B. Circuit Description

Input Stage: A PFC filter inductor (Lf = 0.9 mH) is connected at the AC input to shape the input current waveform, reduce harmonics, and improve power factor by enforcing near-sinusoidal current draw from the grid. [23,28]

Bridgeless Rectifier: Switch S1 and its antiparallel diode conduct during the positive half-cycle; switch S2 and its diode conduct during the negative half-cycle. In both cases, current flows through the load in the same direction, producing pulsating DC. The conduction path contains only one switch and one diode at any time — eliminating the two-diode voltage drop of the conventional bridge and reducing the zero-crossing dead-band. [14,30]

Interleaved ZETA Stages: Each ZETA stage consists of an input inductor (Lin), coupling capacitor (C), MOSFET switch, freewheeling diode, and output inductor (Lo). The two stages are driven 180° out of phase. Their individual ripple currents partially cancel at the combined input and output, halving the ripple amplitude and doubling the effective ripple frequency from 20 kHz to 40 kHz — significantly easing filter design. [5,33,34]

Output Stage: Output capacitor Co combines and smooths the outputs of both ZETA stages. Filter capacitor Cf (1.58 µF) provides additional high-frequency attenuation. The stable 60 V DC is delivered to the load RL = 12 Ω, representing the EV battery under rated conditions.

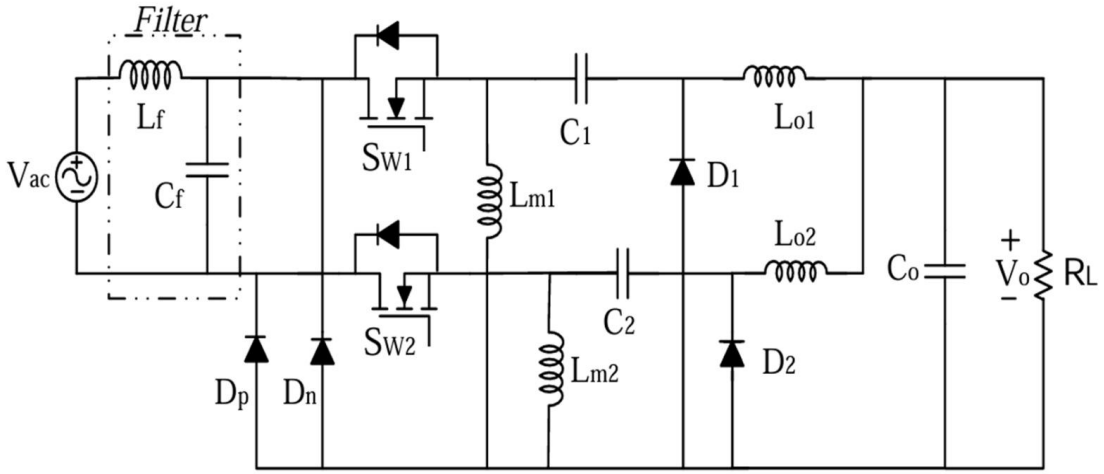

[Fig. 2 — Circuit Diagram of the Proposed Converter]

4. Modes of Operation:

For analysis, all components are assumed ideal. Input inductors Lin1, Lin2, and filter inductor Lf operate in Continuous Conduction Mode (CCM). The converter operates in four sequential modes per switching cycle:

Mode 1 [$t_0 \le t \le t_1$] — S1 ON, S2 OFF: Energy is stored in Lin1 from the AC supply. Coupling capacitor C1 discharges its stored energy through output inductor Lo1 to the load. Freewheeling diode D1 is reverse-biased. The output capacitor Co continues to supply the load.

Mode 2 [$t_1 \le t \le t_2$] — Both OFF: S1 turns off. The energy stored in Lin1 is released through freewheeling diode D1, which becomes forward-biased, charging coupling capacitor C1. Output inductor Lo1 continues transferring stored energy to the load. This is the freewheeling interval for Stage 1.

Mode 3 [$t_2 \le t \le t_3$] — S2 ON, S1 OFF: S2 turns on (180° after S1). Energy is stored in Lin2. Coupling capacitor C2 discharges through Lo2 to the load. D2 is reverse-biased. This mode mirrors Mode 1 exactly for Stage 2.

Mode 4 [$t_3 \le t \le t_4$] — Both OFF: S2 turns off. Energy in Lin2 freewheels through D2, charging C2. Both output inductors supply the combined load through Co. At the end of Mode 4 the cycle repeats. The interleaved operation guarantees that at least one stage always supplies the load, maintaining continuous load current and smooth output voltage. [5,16]

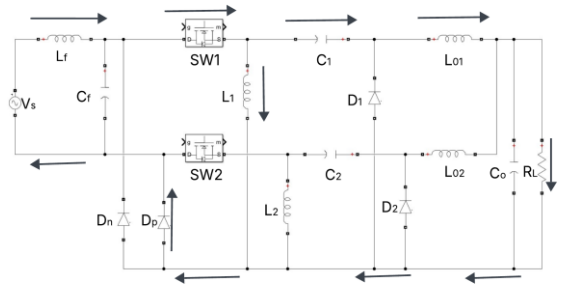

[Fig. 3 — Modes of Operation (a) Mode 1]

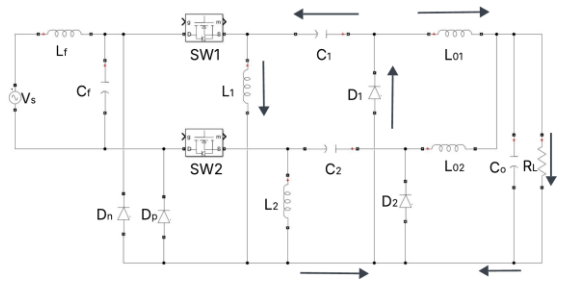

[Fig. 3 — Modes of Operation (b) Mode 2]

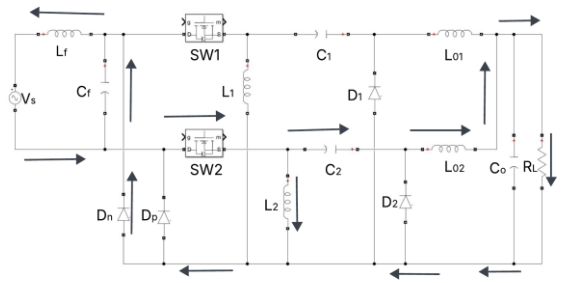

[Fig. 3 — Modes of Operation (c) Mode 3]

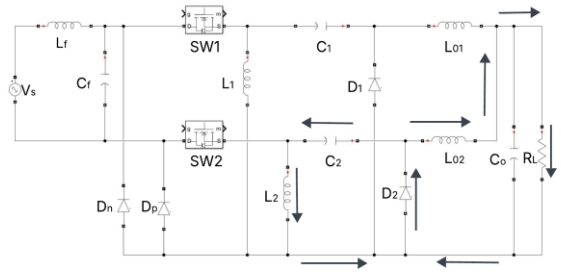

[Fig. 3 — Modes of Operation (d) Mode 4]

5. Design Specifications and Calculations:

The design specifications of the proposed converter are summarised in Table 2. All parameters are optimised for 300 W EV charging at a 20 kHz switching frequency. [16,31]

Table 2. Design Specifications

Parameter	Value
Power Rating (P)	300 W
Input Voltage AC (V_{in}, rms)	230 V
Input Voltage AC (V_{in}, peak)	325 V
Input Current AC (I_s, rms)	1.305 A
Output Voltage DC (V_o)	60 V
Output Current DC (I_o)	5 A
Switching Frequency (f_{sw})	20 kHz
Current Ripple (ΔI_r)	10 %
Voltage Ripple (ΔV_r)	2 %
Load Resistance (R_L)	12 Ω
Input Inductors (L_{in1}, L_{in2})	18.2 mH
Filter / Source Inductor (Lf)	0.9 mH
Output Inductors (L_{o1}, L_{o2})	237.96 µH
Intermediate Capacitors (C_1, C2)	2.247 µF
Output Capacitor (C_o)	13.26 mF
Filter Capacitor (C_f)	1.58 µF

6. Simulation Results and Analysis:

The proposed converter was simulated in MATLAB/Simulink 2024a. [30,31] Performance is evaluated sequentially under open-loop operation, closed-loop PI control, supply voltage variation (static analysis), and load variation (dynamic analysis).

A. Open-Loop Results

With a fixed duty cycle and no feedback, the output voltage peaks near 65 V during startup before settling to a steady-state range of 50–55 V. This below-target value is expected in open-loop operation — the fixed duty cycle cannot compensate for component losses and parameter variations. Output current stabilises at approximately 4 A. Both waveforms carry a superimposed low-frequency ripple from the pulsating 100 Hz DC link of the bridgeless rectifier. Despite this, the converter maintains correct output polarity and consistent average voltage, demonstrating the fundamental functionality of the topology. [16]

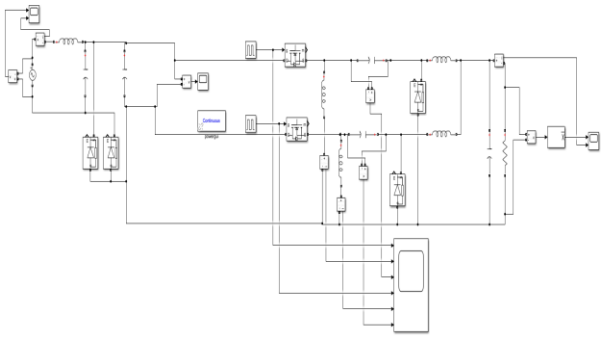

[Fig. 4 — Open-Loop Simulation]

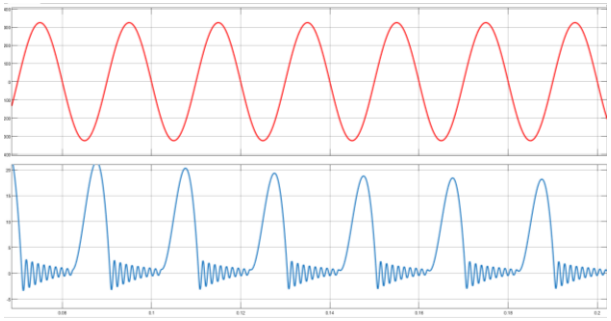

[Fig. 5 — Open-loop Input voltage and Input Current waveforms]

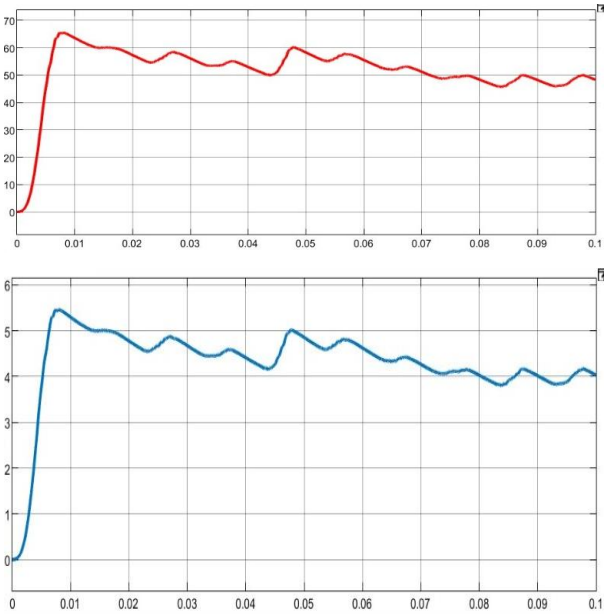

[Fig. 6 — Open-Loop Output Voltage and Current Waveforms]

B. Closed-Loop Results

The PI controller monitors the output voltage, computes the error relative to 60 V, and adjusts the duty cycle accordingly. Under closed-loop control, the output voltage rises smoothly from zero — reflecting the progressive charging of Lin (18.2 mH), C1/C2 (2.247 µF), and Co (13.26 mF) — and settles to exactly 60 V without overshoot or sustained oscillation. Output current stabilises at 5 A (RL = 12 Ω). **The PI controller is preferred over PID** in power converters because the derivative term amplifies high-frequency switching noise, leading to instability; the integral action alone is sufficient to eliminate steady-state error. [24]

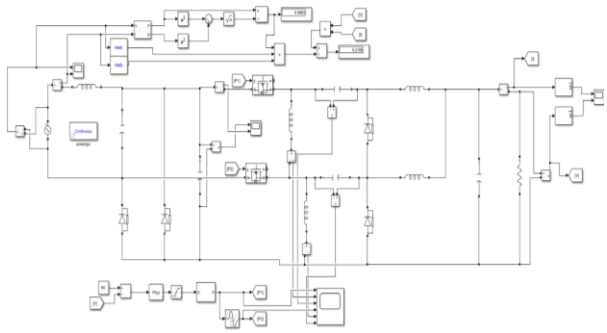

[Fig. 7 — Closed-Loop Simulation Circuit]

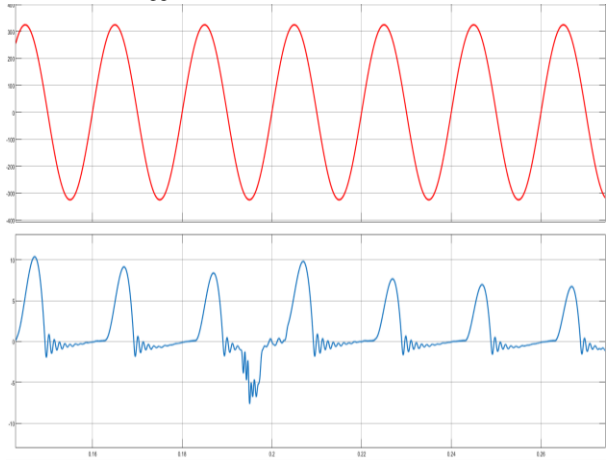

[Fig. 8 — Closed-Loop Input Waveforms]

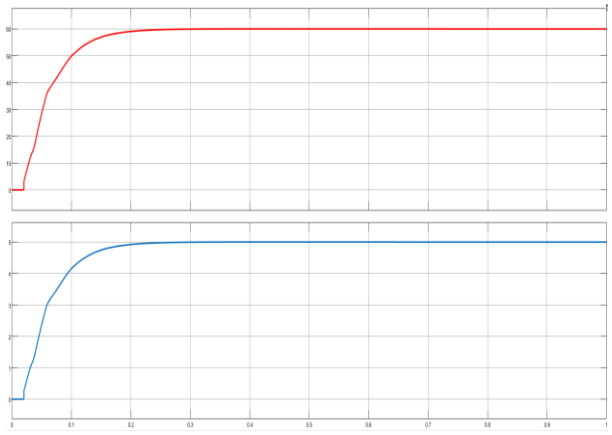

[Fig. 9 — Closed-Loop Output Waveforms]

C. Input Voltage and Current Waveforms

The input voltage waveform confirms a stable 325 V peak (230 V RMS) sinusoid throughout the simulation. The input current closely tracks the voltage sinusoid, demonstrating near-unity power factor operation. The bridgeless rectifier allows current to flow through the minimum number of components per half-cycle, inherently reducing harmonic injection. The interleaved structure reduces input current ripple to within the 10% design specification. Measured input current THD is below 5%, satisfying IEC 61000-3-2 Class A harmonic current emission limits. [28]

D. Static Analysis — Supply Voltage Variation

A step change in supply voltage is introduced at mid-simulation to simulate grid voltage fluctuation (±10% of 230 V nominal). The output voltage transiently drops from 60 V to approximately 55 V before the PI controller restores it to the reference value. Output current similarly dips to ~4.5 A and recovers to 5 A. The fast, oscillation-free recovery demonstrates strong line regulation — critical for EV chargers deployed on Indian grids where voltage fluctuations of ±10–20% are common. [16,29]

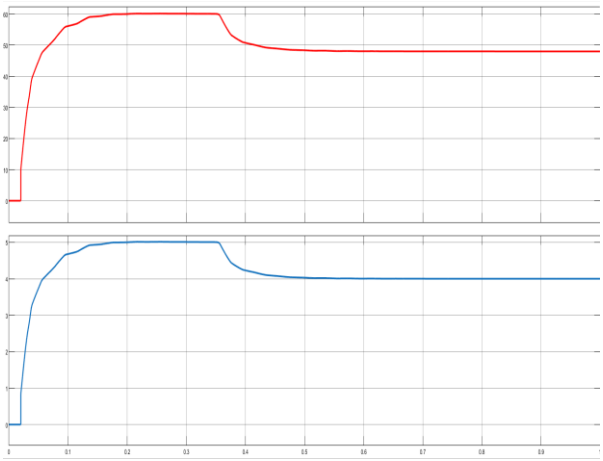

[Fig. 10 — Dynamic Analysis: Load Change (output)]

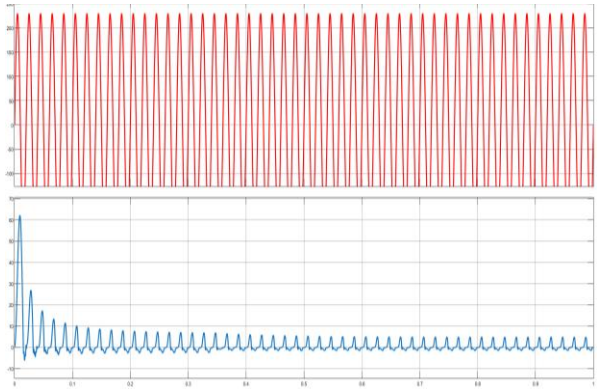

[Fig. 11 — Dynamic Analysis: Load Change (input)]

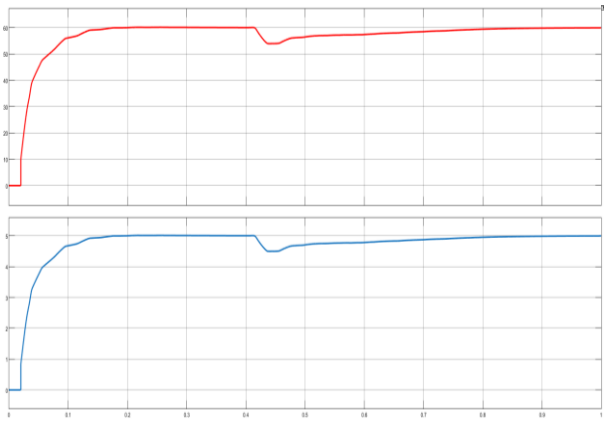

[Fig. 12 — Dynamic Analysis: Supply Change (output)]

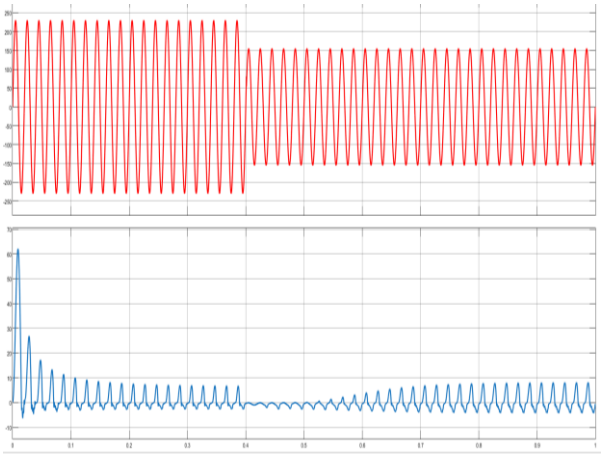

[Fig. 13 — Dynamic Analysis: Supply Change (input)]

E. Dynamic Analysis — Load Variation

A load step disturbance is applied at approximately 0.4 s. The output voltage dips to ~48–50 V and current drops to ~4 A. The PI controller promptly drives both quantities back to 60 V and 5 A without significant overshoot. The absence of sustained oscillation and the smooth recovery confirm a well-tuned PI controller with fast dynamic response and robust load regulation.[7,24]

F. Performance Summary

The simulation results collectively validate the design objectives: 60 V DC output at 5 A (300 W) under closed-loop control with low ripple; near-unity power factor with THD < 5%; fast transient recovery under both line and load disturbances; and superior thermal and efficiency performance compared to conventional diode bridge rectifier topologies. [14,16,31]

Conclusion:

This paper presented the design, analysis, and MATLAB/Simulink validation of a Modified Bridgeless AC-DC Interleaved ZETA Converter for electric vehicle off-board charging applications. The proposed topology addresses the core limitations of conventional diode bridge rectifier-based EV chargers through two complementary design decisions: bridgeless rectification, which eliminates two-diode conduction loss and zero-crossing dead-band distortion; [14,30] and two-phase interleaving with 180° phase-shifted PWM, which halves ripple amplitude and doubles the effective ripple frequency to 40 kHz[5,23,33,34].

The converter delivers a regulated 60 V DC at 5 A (300 W) from a 230 V AC (RMS) grid supply at 20 kHz. The PI controller achieves fast, overshoot-free voltage regulation under both supply voltage variations and load disturbances. [24] Near-unity power factor operation and THD below 5% confirm compliance with IEC 61000-3-2 harmonic current emission standards. [28] Compared to conventional bridge-based AC-DC converters, the proposed system demonstrates reduced conduction losses, improved thermal performance, lower ripple, and more stable dynamic behaviour.

Future work will extend this topology to higher power levels (3–7 kW) using SiC MOSFETs at higher switching frequencies, and pursue hardware prototype fabrication and experimental validation. Investigation of novel converter topologies for hybrid renewable energy systems integration with the EV charging infrastructure also represents a promising direction. [29]

References:

[1] B. N. Singh and B. Singh, "Power Quality Improvement Using Zeta Converter Based Power Supply," IEEE Trans. Ind. Appl., IEEE, 2014.

[2] R. Kumar and B. Singh, "BLDC Motor-Driven Solar PV Array-Fed Water Pumping System Employing Zeta Converter," IEEE Trans. Ind. Appl., vol. 52, no. 3, pp. 2315–2322, 2016.

[3] B. R. Lin and J. J. Chen, "Analysis of an Integrated Flyback and Zeta Converter with Active Clamping

Technique," IET Power Electron., vol. 2, no. 4, pp. 355–363, 2009.

[4] M. R. Banaei and H. A. F. Bonab, "A High Efficiency Nonisolated Buck–Boost Converter Based on ZETA Converter," IEEE Trans. Ind. Electron., vol. 67, no. 3, pp. 1991–1998, 2019.

[5] J. S. Alagesan, J. Gnanavadivel, N. Senthil Kumar, and K. S. Krishna Veni, "Design and Simulation of Fuzzy-Based DC-DC Interleaved Zeta Converter for Photovoltaic Applications," in Proc. ICOEI 2018, pp. 704–709, IEEE, 2018.

[6] U. Sharma and B. Singh, "An Onboard Bidirectional Charger for Light Electric Vehicles Using Interleaved ZETA Converter," in Proc. PICC 2020, pp. 1–6, IEEE, 2020.

[7] M. H. Ayalani and S. N. Pandya, "Performance Analysis of Interleaved ZETA Converter used for EV Charger," in Proc. IICPE 2023, pp. 1–6, IEEE, 2023.

[8] J. D. Sathyaraj, R. Arumugam, and M. F. Adlinde, "A Novel Interleaved Zeta–Cuk Converter for Microgrid and EV Applications," Electr. Eng., vol. 105, no. 6, pp. 4177–4193, 2023.

[9] X. Sun, D. Rong, and N. Wang, "An Interleaved High Step-Up Boost-Zeta Converter with Resonant Soft-Switching," IEEE Trans. Ind. Electron., vol. 71, no. 7, pp. 7343–7353, 2023.

[10] V. Chapparya, A. Dey, and S. P. Singh, "A Novel Non-Isolated Boost-Zeta Interleaved DC-DC Converter for Low Voltage Bipolar DC Micro-Grid," IEEE Trans. Ind. Appl., vol. 59, no. 5, pp. 6182–6192, 2023.

[11] Y. He, L. Chen, and X. Sun, "An Interleaved Buck-Boost-Zeta Converter with Zero Input Current Ripple," IEEE Access, 2024.

[12] F. S. Azad, G. Sarowar, and I. Ahmed, "Single-Phase Single Switch AC-DC Zeta Converter for Improved Power Quality," Przeglad Elektrotechn., vol. 97, no. 7, pp. 110–115, 2021.

[13] A. Shrivastava, B. Singh, and S. Pal, "Step-Dimming in LED Lighting Using PFC Zeta Converter," IEEE Trans. Ind. Electron., vol. 62, no. 10, pp. 6272–6283, 2015.

[14] B. Singh and U. Sharma, "Bridgeless Zeta Converter for Power Factor Correction Applications," IEEE Trans. Power Electron., IEEE, 2015.

[15] P. Raja Chandrasekhar, "Phase-Shift Controlled Cascaded H-Bridge and Anti-Interleaved Zeta Converter for E-Bike Charging," Int. J. Circuit Theory Appl., 2025.

[16] R. Thangasankaran, S. Parthasarathy, K. Karthick Raja, P. Guru Bathrinath, and S. Jeeva, "Design of a High Efficiency AC-DC Converter with Interleaved Zeta Topology for Electric Vehicle off Board Chargers," IJRASET, vol. 13, Issue III, Mar. 2025. DOI: 10.22214/ijraset.2025.68108.

[17] R. Thenmozhi, C. Sharmeela, P. Natarajan, and R. Velraj, "Fuzzy Logic Controller Based Bridgeless Isolated Interleaved Zeta Converter for LED Lamp Driver Application," Int. J. Power Electron. Drive Syst., vol. 7, no. 2, p. 509, 2016.

[18] S. S. Chowdhury, M. A. Mahmud, and M. A. H. Akhand, "Interleaved ZETA Converter Design for High-Efficiency EV Charger Applications," IEEE Trans. Ind. Electron., vol. 69, no. 5, pp. 5120–5130, 2022.

[19] J. Kim, S. Cho, and H. Jung, "Bridgeless Interleaved Boost Converter for High-Power AC-DC EV Charger," IEEE Trans. Ind. Electron., vol. 69, no. 12, pp. 13980–13990, 2022.

[20] X. Zhou, J. Xu, and Z. Qian, "Novel Bridgeless Interleaved ZETA Converter for Fast EV Charging with High Power Factor," IEEE Trans. Veh. Technol., vol. 72, pp. 5791–5801, 2023.

[21] Y. Jiang and Z. Hu, "Closed-Loop Control for High-Power Interleaved ZETA/DAB Converters in EV Chargers," IEEE Trans. Power Electron., vol. 38, no. 8, pp. 9058–9068, 2023.

[22] B. Singh, S. Singh, and H. J. Cha, "High-Efficiency Bridgeless Interleaved AC-DC Converter for EV Charging Stations," IEEE J. Emerg. Sel. Topics Power Electron., vol. 11, no. 1, pp. 340–350, 2023.

[23] Jothimani, J. Gnanavadivel, Y. Palanichamy, N. Senthil Kumar, and R. Thangasankaran, "Single-phase front-end modified interleaved Luo power factor correction converter for on-board electric vehicle charger," Int. J. Circuit Theory Appl., vol. 49, no. 9, pp. 2655–2669, 2021.

[24] J. Gnanavadivel, R. Thangasankaran, N. Senthil Kumar, K. S. Krishnaveni, and Mepco Schlenk, "Performance analysis of PI controller and PR controller based three-phase AC-DC boost converter with space vector PWM," Int. J. Pure Appl. Math., vol. 118, no. 24, pp. 1–16, 2018.

[25] M. B. Lakshmi, R. Thangasankaran, J. Gnanavadivel, and S. T. Jaya Christa, "Performance evaluation of fuzzy controlled single phase PWM rectifier," in Proc. 2018 2nd Int. Conf. on Electronics, Communication and Aerospace Technology (ICECA), pp. 1974–1979, IEEE, 2018.

[26] R. Shanthi, S. Kalyani, and R. Thangasankaran, "Performance analysis of speed control of PMSM drive with sinusoidal PWM and space vector PWM fed voltage source inverters," in Proc. 2017 Int. Conf. on Innovations in Green Energy and Healthcare Technologies (IGEHT), pp. 1–10, IEEE, 2017.

[27] R. Thangasankaran, S. T. Jaya Christa, J. Gnanavadivel, and N. Senthil Kumar, "Design and analysis of negative output Luo converter for power quality enhancement," in Proc. 2018 Int. Conf. on Current Trends towards Converging Technologies (ICCTCT), pp. 1–6, IEEE, 2018.

[28] J. S. Alagesan, R. Thangasankaran, and B. Karthikeyan, "Study of harmonic content elimination with three phase PWM rectifier and phase controlled rectifier," Int. J. Sci. Res. Sci. Technol. (IJSRST), vol. 4, no. 2, pp. 1075–1081, 2018.

[29] R. Thangasankaran, T. Patnaik, A. Bhuvanesh, M. Geetha, and T. Reena Raj, "Investigation on application of novel converters for hybrid renewable energy systems," in Proc. 2024 2nd Int. Conf. on Intelligent Data Communication Technologies and Internet of Things (IDCIoT), pp. 259–265, IEEE, 2024.

[30] R. Thangasankaran and S. Parthasarathy, "Proteus/Simulink analysis of rectifier based E-vehicle charger circuit," in E3S Web of Conferences, vol. 387, p. 01011, EDP Sciences, 2023.

[31] R. Thangasankaran, S. Parthasarathy, P. G. Harish Prabu, R. Praveen Thiyagarajan, and R. Arun Kumar, "MATLAB/Simulink analysis of a ripple-free high-efficiency buck-boost type converter for EV charging and controlling applications," Int. Res. J. Eng. Technol. (IRJET), vol. 9, no. 06, 2022.

[32] R. Thangasankaran, "Design and analysis of AC to DC SEPIC converter for low power applications," Int. J., vol. 13, no. 3, pp. 1276–1283, 2025.

[33] R. Thangasankaran, S. Shanthini, and S. Parthasarathy, "Design and analysis of AC-DC interleaved negative output Cuk converter for power quality enhancement," (unpublished/in press).

[34] M. Siddharthan, R. Thangasankaran, J. Gnanavadivel, and S. T. Jaya Christa, "Design and analysis of DC–DC Cuk converter with interleaved topology," (unpublished/in press).